RMetS

Royal Meteorological Society

Understanding and attributing the Euro-Russian summer blocking signatures

Paolo M. Ruti,[1] A. Dell'Aquila[1]* and F. Giorgi[2]

[1]*UTMEA-CLIM Energy Environment Modeling Unit – Climate & Impact Modeling Laboratory, ENEA, Rome, Italy*
[2]*Earth System Physics Section, ABDUS SALAM ICTP, Trieste, Italy*

*Correspondence to:
A. Dell'Aquila, UTMEA-CLIM
Energy Environment Modeling
Unit – Climate & Impact
Modeling Laboratory, ENEA,
Rome, Italy.
E-mail:
alessandro.dellaquila@enea.it*

Abstract

In this work, we focus on summer blocking events over the Euro-Russian region related with heat waves. An analysis of the main characteristics of summer Euro-Russian blocking events in global Reanalysis as well as in the 20th century CLIVAR atmospheric simulations is carried out to assess whether anthropogenic forcing might have affected the blocking events occurrence and the associated heat waves strength in recent decades. Over the Euro-Russian region, blocking episodes, associated to warm events over Northern and Central Europe, become significantly longer in the second half of the century when the anthropogenic forcing is included in the simulations.

Keywords: **Euro-Russian summer blocking; anthropogenic forcing; historical climate simulations**

1. Introduction

The recent European heat waves of summer 2003 and 2010 have received considerable attention because of both their potential link to larger scale warming patterns (e.g. 'global warming') and the large loss of life and resources associated with them (Black *et al.*, 2004; Barriopedro *et al.*, 2011). Understanding and quantifying how anthropogenic climate change might affect the intensity and frequency of extreme events has become a priority in climate studies. In particular, it has been suggested that increases in extreme events such as heat waves could be explained by increased temperature variability (Schär *et al.*, 2004; Fischer *et al.*, 2012). These heat waves have been associated mainly to the low-frequency component of the atmospheric flow, and specifically to long-lived blocking episodes (Cassou *et al.*, 2005; Dole *et al.*, 2011). It is thus possible that trends in the occurrence and strength of heat waves might be in fact related to corresponding trends in blocking patterns. However, this point remains a debating issue: for instance, Cattiaux *et al.* (2012) have found weak links between simulated changes in temperature extremes in Europe and changes in circulation. Starting from these considerations, here we investigate whether trends in blocking episodes occurrence and length during the last decades, along with the eventual consequences on strength of associated warm events, can be attributed to anthropogenic forcing or are simply associated with the natural variability of the climate system.

Blocking diagnostics have been widely used both in forecast models (Anderson, 1993; Ferranti *et al.*, 1994; Tibaldi *et al.*, 1995; Jung, 2005) and in climate simulations (Lupo *et al.*, 1997; D'Andrea *et al.*, 1998; Doblas-Reyes *et al.*, 2002; Matsueda *et al.*,

2009; Vial and Osborn, 2011; Dunn-Sigouin and Son, 2013). Such local blocking diagnostics, together with time–space spectral decomposition of mid-latitudes variability (Dell'Aquila *et al.*, 2005) and with the adoption of global indicators for planetary waves activity (Hansen and Sutera, 1986; Corti *et al.*, 1999; Ruti *et al.*, 2006 among others), are powerful analysis tools which can be readily applied to daily data of the 500 hPa geopotential height in order to identify relevant blocking patterns. In this article, we thus apply blocking diagnostics to the output of Global Climate Model (GCM) simulations for the 20th century with and without anthropogenic forcings (Greenhouse gas (GHG) changes, atmospheric ozone change, sulphate aerosols and land surface changes) to investigate their role in modifying the occurrence and characteristics of relevant blocking events and associated heat waves over recent decades.

2. Data and methods

We analyse two ensembles of six integrations performed with the Hadley Centre Atmospheric Model 3 (hereafter HadAM3) global atmospheric model for the period 1869–2002 available from the CLIVAR C20C and EMULATE projects website (http://hadc20c.metoffice.com/). In all simulations, the Met Office Hadley Centre's sea ice and sea surface temperature (SST) data set, HadISST1, has been included (Rayner *et al.*, 2003). In the first ensemble of simulations (hereafter referred to as 'NATURAL') only natural forcings are included, namely SST, volcanic aerosols, solar variability and orbital changes. In
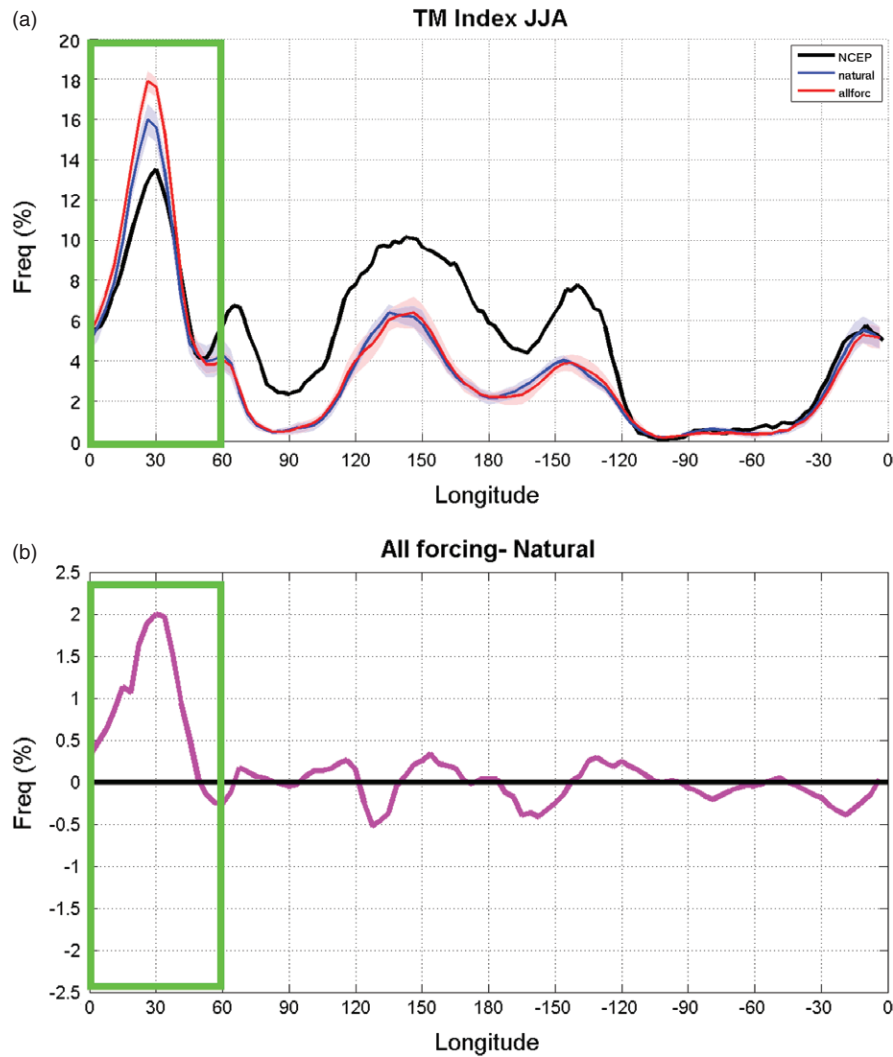
Figure 1. (a) Frequency of summer days that are part of large-scale blocking episodes as a function of longitude for the 'NATURAL' (blue curve) and 'ALLFORCINGS' simulations (red curve) for 1901–2000 period. The shaded corresponding regions are for the ensembles spread (±1 standard deviation). The thick black line reports the reference curve from NCEP global Reanalysis dataset (1961–2010). The green box is for the Euro-Russian sector (0°–60°E). (b) Differences in frequency of blocked days between ALLFORCINGS and NATURAL experiments.

the second set, (hereafter referred to as 'ALLFORC-INGS') the model includes, in addition to the natural forcings, anthropogenic forcings associated with greenhouse gas changes (as appears in the web site http://hadc20c.metoffice.com) and atmospheric ozone changes, sulphate aerosols and land-use change (major details in the web site and in the technical report there reported). The use of the labels 'NATURAL' and 'ALL-FORCINGS' could be potentially misleading, since the two ensembles of simulations use the same specified observed SST and sea ice conditions, which can already include some effects of anthropogenic forcings. So our analysis could not fully separate the natural and anthropogenic forcings, and in particular disentangle its effects on ocean and sea ice. However, with this caveat in mind, in order to keep this work consistent with terms adopted by the C20C project, we here follow the definitions presented in http://hadc20c.metoffice.com. Records of daily 500-hPa geopotential height for the 100-year long period (1901–2000) were extracted

along with corresponding fields from the National Centers for Environmental Prediction-National Center for Atmospheric Research (NCEP-NCAR) global Reanalysis dataset (1961–2010) as reference.

Our blocking detection method is based on the index of Tibaldi and Molteni (1990), which identifies atmospheric blocking highs when easterlies are present in the regions of maximum interactions between storm tracks and mean flow (Carillo *et al.*, 2000). At each longitude, we compute the southern and the northern 500 hPa gradient, defined as GHGS and GHGN, respectively:

$$\mathrm{GHGS} = \left[\frac{Z\left(\phi_0\right) - Z\left(\phi_s\right)}{\phi_0 - \phi_s} \right]$$

$$\mathrm{GHGN} = \left[\frac{Z\left(\phi_n\right) - Z\left(\phi_0\right)}{\phi_n - \phi_0} \right] \quad (1)$$

where $\phi_0 = 60°\mathrm{N} + \Delta$; $\phi_s = 40°\mathrm{N} + \Delta$; $\phi_n = 80°\mathrm{N} + \Delta$ and $\Delta = [-5°; 0; 5°]$.

A given longitude is blocked if the following conditions are satisfied for at least one value of Δ

1 GHGS > 0
2 GHGN < -10 m/degree latitude

We apply a 5-day running mean to the geopotential height field and focus on the summer season (June-July-August, JJA).

3. Results

We first analyse the summer blocking frequency in the 1901–2000 period for the 'NATURAL' and 'ALLFORCINGS' simulations (Figure 1). There are two main regions of blocking development: the Euro-Russian (0°–60°E), which is bounded by the Ural Mountains, and the Pacific (90°E–120°W).

Compared to the 1961–2010 NCEP data (black thick line), HadAM3 is able to capture all peaks, although it underestimates the Pacific frequency and overestimates the European frequency. The higher frequency of blocking events over the Atlantic region may be due to the fact that SST errors generally present in coupled models over Atlantic Ocean are here removed (Scaife et al., 2011). The 'ALLFORCINGS' simulations differ significantly from the 'NATURAL' ones just over the Euro-Russian sector where the 'ALLFORCINGS' ensemble is well separated from 'NATURAL' simulations (Figure 1(a)). As reported in Figure 1(b), the Euro-Russian sector (0°–60°E) is the only region showing a systematic increase of frequency of blocking days in the 'ALLFORCINGS' simulations with respect to the 'NATURAL' ones.

In order to investigate the differences between the two ensembles, we distinguish between changes in the number and duration of blocking events. We have computed the number of blocking events for each summer season over the Euro-Russian sector, together with the corresponding interannual variability (i.e. the standard deviation). Results for the two ensembles are shown in Figure 2, along with the corresponding number occurrence in the NCEP global Reanalysis dataset. The number of summer blocking episodes per season does not show significant differences between the 'NATURAL' and 'ALLFORCINGS' mean ensembles. We also find that HadAM3 is able to capture the averaged blocking episodes number when compared with the NCEP data. In addition, the interannual variability of the number of events per season is quite similar for each considered dataset.

In order to determine the main source of differences between the two ensembles in Figure 1, we computed the Probability Distribution Function (PDF) of the length in days of the Euro-Russian blocking episodes. Figure 3(a) presents PDF of length of blocking events for each ensemble, along with the difference between the 'NATURAL' and 'ALLFORCINGS' experiments (Figure 3(b)). Additional explanations concerning the computation of the PDF are in the caption of
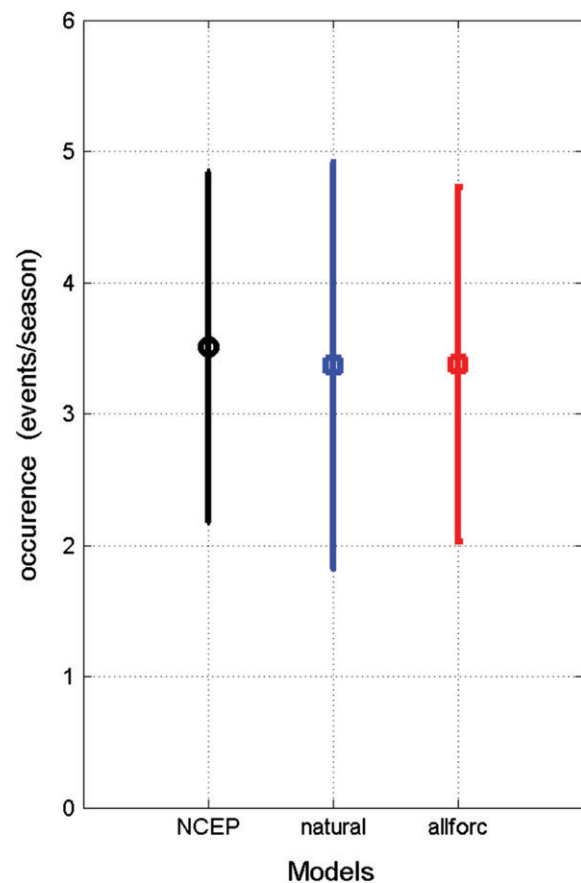

Figure 2. Number of blocking events for season over Euro-Russian sector. The ensembles mean results for the 'NATURAL' (blue bar) and 'ALLFORCINGS' simulations (red bar) are shown over the 1901–2000 period. The vertical bars show the interannual variability of the occurrence for each ensemble (± 1 standard deviation). The black bar reports the occurrence in the NCEP global Reanalysis dataset (1961–2010) with the associated interannual variability.

Figure 3(a). The 'ALLFORCINGS' experiments exhibit a tendency to generate longer blocking events, especially in the range of 5–15 days, which in turn explains the higher blocking day occurrence observed in Figure 1. A Kolmogorov–Smirnov (KS) test applied to the lengths of blocking events in the two ensembles confirms that they are from different continuous distributions (KS = 1 in Figure 3(b)). To better highlight this aspect, we analysed the length of blocking events separately for two different subperiods: (1901–1950), when the anthropogenic forcing is relatively small, and (1951–2000) when the anthropogenic forcing sharply increases (e.g. IPCC, 2001) (Figure 3(c)–(f)). In the first period, the distributions of the blocking length are statistically undistinguishable at the 99% confidence level between the 'NATURAL' and 'ALLFORCINGS' experiments (Figure 3(c) and (d)). On the other hand, different lengths of blocking events in the two sets of experiments characterize mostly the period 1951–2000 (Figure 3(e) and (f)). In the second half of the 20th century, the blocking events in the 'ALLFORCINGS' simulations tend to be considerably longer with respect to the beginning of the century, whereas the length
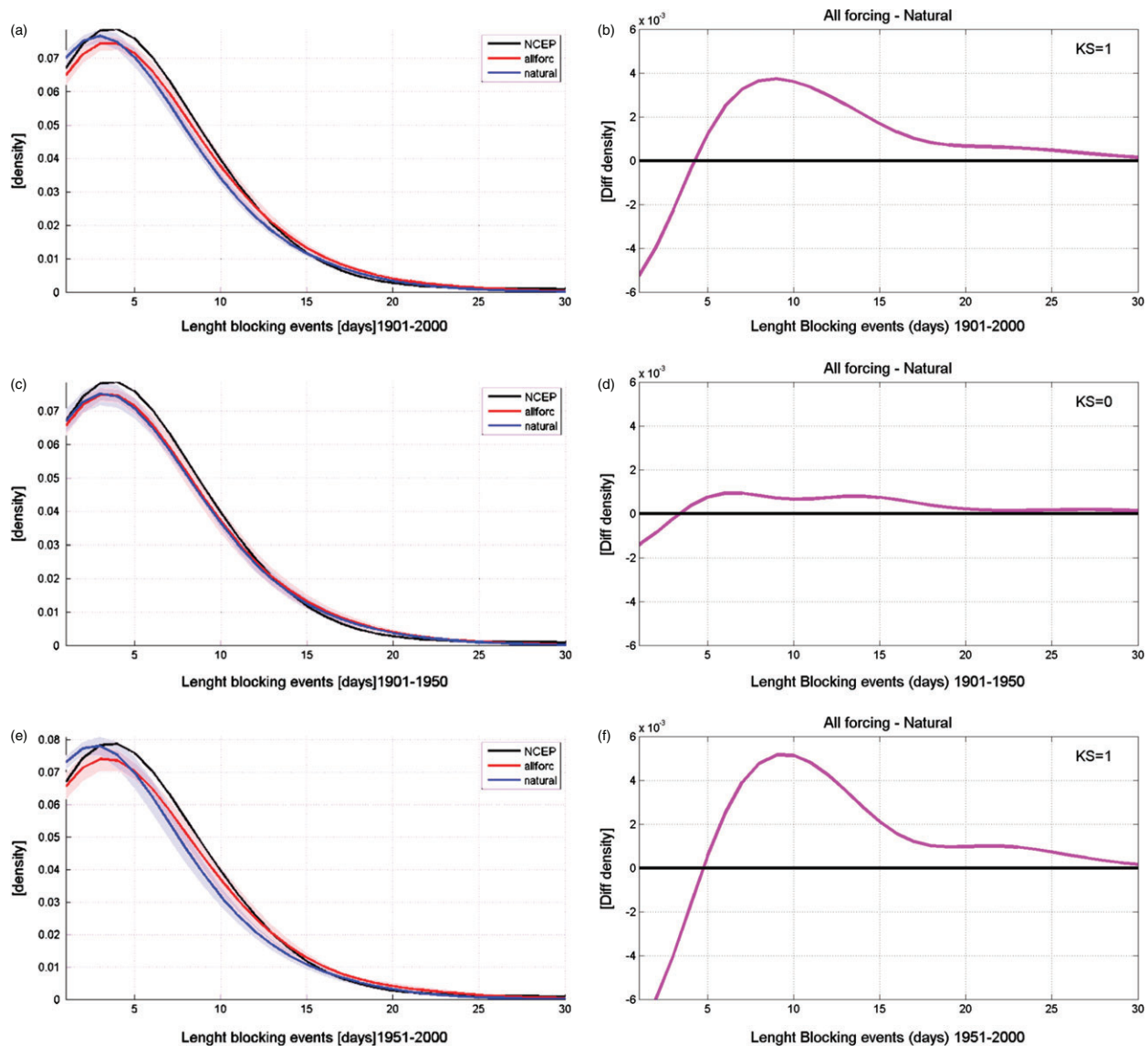
Figure 3. (a) PDF of length (in days) of Euro-Russian blocking events for the period 1901–2000. Results from the two ensembles for the 'NATURAL' (blue curve) and 'ALLFORCINGS' (red curve) simulations are shown. The corresponding shaded regions are for the spread of each ensemble (±standard deviation). The thick black line reports the occurrence in the NCEP global Reanalysis dataset. PDF's are computed by adopting a Gaussian kernel function estimator and by using a window parameter $h = 3.5*\Delta$, where Δ is the bin amplitude. We assume 100 bins in the interval between the minimum and maximum length. (b) Difference of PDFs for the length of blocking events between 'NATURAL' and 'ALLFORCINGS' experiments for 1901–2000 period. If the Kolmogorov–Smirnov test (KS) = 1, the differences in the length of blocking events are significant at the 99% confidence level (KS = 0 otherwise). (c, d) As in (a) and (b) but for 1901–1950 period. (e, f) As in (a) and (b) but for 1951–2000 period.

of the events in the 'NATURAL' simulations remains basically unchanged. A tendency towards longer blocking events can also be recognized in NCEP reanalysis considering different periods (1991–2010 compared against 1961–1980) even if not statistically significant due to the small size of samples (Figure S1, Supplementary Information). Evidence and possible explanations of the recent increase in summer blocking and weather extremes have been recently presented in Petoukhov *et al.* (2013), where a mechanism of amplification of planetary waves linked to the structure of subtropical jet has been presented. In this perspective, the anthropogenic forcing could lead to an increase of weather extremes by modifying the mean thermal structure of mid-latitudes atmosphere.

In order to provide evidence of the link between blocking episodes and high temperatures, we composited the surface air temperature during blocking events. We consider blocking events longer than 10 days, to explore cases that can favour the establishment of a heat wave, as in 2010 (Dole *et al.*, 2011). In Figure 4, we report maps of surface air temperatures anomalies (with respect to the corresponding climatological mean) for blocking events longer than 10 days in NCEP (Figure 4(a)) as well as in 'ALLFORCINGS' and 'NATURAL' simulations (Figure 4(b) and (c)), respectively. For HadAM3 simulations, we consider the period 1951–2000 where the main differences in the length of blocking events arise (Figure 3(e) and (f)). Shading areas denote that composite anomalies are statistically
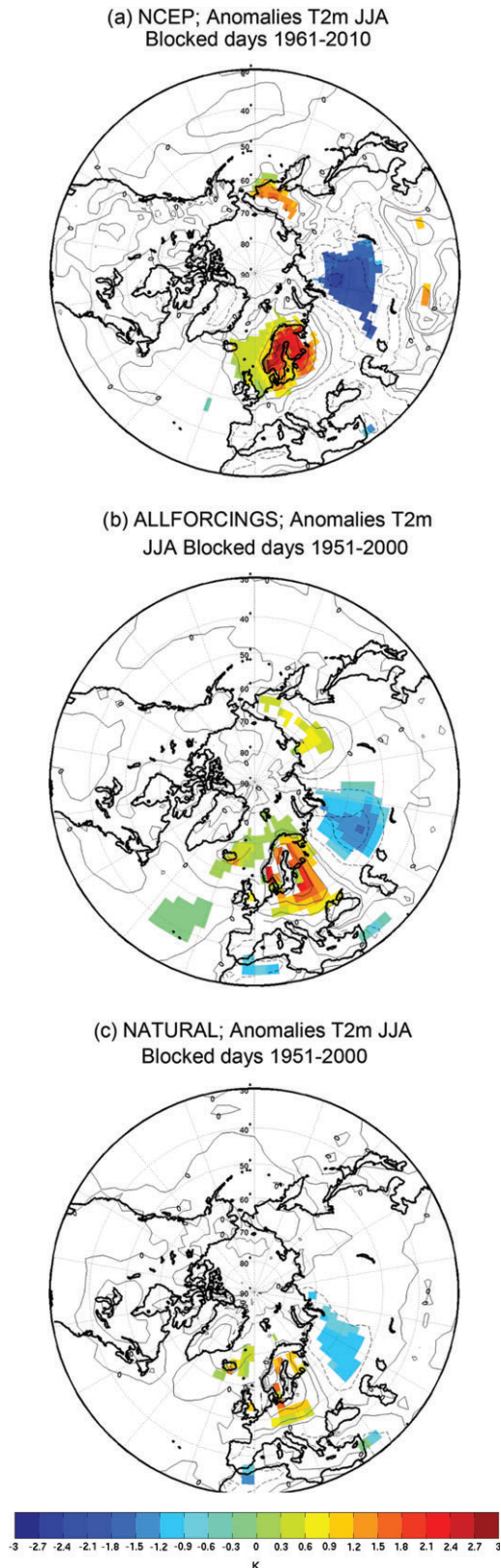
Figure 4. Maps of surface air temperature anomalies (with respect to the corresponding climatological mean) over during summer blocking events longer then 10 days. (a) NCEP global Reanalysis dataset (1961–2010). (b) 'ALLFORCINGS' simulations (1951–2000). (c) 'NATURAL' simulations (1951–2000). In the filled regions, the differences are statistically significant at 90% level (t-test). Solid contours are for positive anomalies, dashed contours for negative values.

significant at the 90% level (t-test). In the NCEP reanalysis (Figure 4(a)), a coherent positive anomaly is seen in the Scandinavian and Euro-Russian region along with a negative anomaly over much of Central Asia and over Southern Europe (not statistically significant). The warming anomaly, even if not statistically significant, reaches also the British Isles and Central Europe. A quite similar structure is well depicted also in 'ALLFORCINGS' simulations (Figure 4(b)) whereas the pattern is still present but weaker in 'NATURAL' ensemble. This suggests that anthropogenic forcings, such as land-use changes, aerosols and greenhouse gases (taken into account in the 'ALLFORCINGS' simulations), are key ingredient in strengthening the surface temperature anomalies during blocking events.

We further analysed the link between blocking events and heat waves by considering the temperature anomalies over a box covering part of the Euro-Russian region (Longitude = 20°–50°E; Latitude = 40°–65°N). In Figure 5, we report the PDF of summer surface air temperature anomalies (with respect to the corresponding climatological mean) over this box for the three datasets (NCEP 1961–2010, 'ALLFORCINGS' 1951–2000 and 'NATURAL' 1951–2000). Solid lines represent temperature anomalies during blocking events longer than 10 days, whereas dotted lines represent non-blocked days. We also report in the legend the mean values and standard deviation for each distribution.

In the NCEP reanalysis, the probability distribution function of surface temperature during blocked days (thick solid black line) is clearly shifted towards warmer temperatures with respect to non-blocked days (with a shift of about 1 K in terms of mean values). Warm events with temperature positive anomalies exceeding 2 K are definitely more populated. In 'ALLFORCINGS' simulations (red curve), the behaviour is quite similar even if the shift of mean values is around 0.5 K. In the 'NATURAL' simulations (blue curve), the shift in the distribution is less evident, highlighting the fact that anthropogenic forcing is needed in order to explain the shift observed in the NCEP reanalysis. Over Northern and Central Europe, the anthropogenic forcing triggers and amplifies the link between blocking episodes and heat waves, at least in terms of surface temperature anomalies.

4. Summary and discussion

Our main results can be summarized as follows:

- Generally, the HadAM3 model simulations capture the observed blocking occurrence, but these runs tend to overestimate the occurrence of summer blocking episodes compared to NCEP over the Euro-Russian sector (0°–60°E).
- In this sector, the 'NATURAL' and 'ALLFORCINGS' experiments feature different numbers of blocked days, and in particular, the 'ALLFORCINGS' simulations show a higher number of blocked
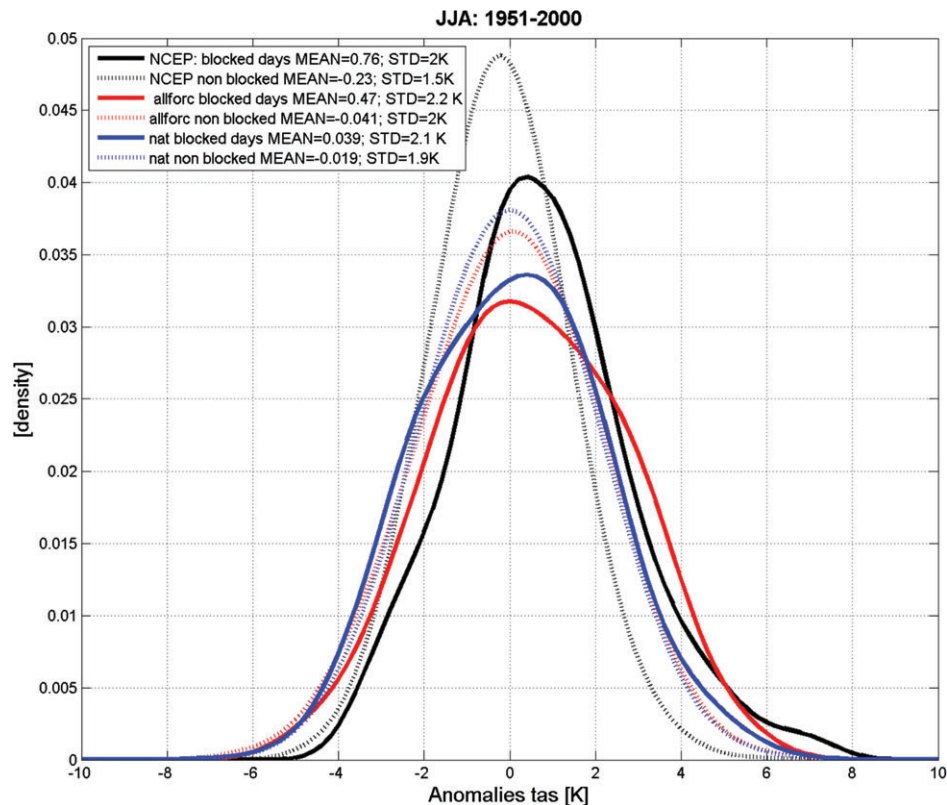
Figure 5. PDF of surface air temperature anomalies (with respect to the corresponding climatological mean) over a box covering part of Euro-Russian region (Longitude = 20°–50°E; Latitude = 40°–65°N) for the period 1951–2000. Solid lines are for surface air temperature anomalies during blocked events longer than 10 days, whereas the dotted lines are for non-blocked days. The black lines are for NCEP global Reanalysis dataset (1961–2010). Blue (Red) line for 'NATURAL' ('ALLFORCINGS') runs. PDF's are computed by adopting a Gaussian kernel function estimator and by using a window parameter $h = 3.5*\Delta$, where Δ is the bin amplitude. We assume 100 bins in the interval between the minimum and maximum length.

days (Figure 1). No significant differences in blocking characteristics between the NATURAL and ALLFORCINGS ensembles are found in regions out of the Euro-Russian sector.

- The frequency of occurrence of Euro-Russian blockings (typically slightly more than 3 events/season) is not affected by inclusion of the anthropogenic forcings (GHG changes, atmospheric ozone change, sulphate aerosols and land-surface changes) (Figure 2), whereas the 'ALLFORCINGS' simulations are characterized by longer lasting blocking events.
- This signature is particularly evident in the second half of the century (Figure 3), when the anthropogenic forcing is larger. Similar behaviour, even if not statistically significant, can be recognized also in the NCEP Reanalysis where the blocking events in the period 1990–2010 are generally longer than in the period 1960–1980.
- The blocking events detected are associated with positive air surface temperature anomalies over Northern and Central Europe in NCEP Reanalysis as well as in 'ALLFORCINGS' simulations. In 'NATURAL' simulations the link between blocking events and heat waves is present but weaker (Figures 4 and 5).
- Our analysis suggests that anthropogenic forcing might indeed affect the characteristics of blocking events in the Euro-Asia sector, in particular

leading to longer blocking episodes, at least in the HadAM3 model 20th century simulations. This can in turn enhance the severity of heat waves associated to blocking over this region, further intensifying episodes such as that which occurred in the summer of 2010 over European Russia (Dole *et al.*, 2011). The anthropogenic forcing is clearly increasing the link between blocking episodes and heat waves, in terms of surface temperature anomalies, over the Euro-Russian region. However, changes in heat wave duration and strength is likely be dominated by land surface feedbacks (Atlas *et al.*, 1993; Fischer *et al.*, 2007). Further studies should investigate the underlying mechanisms that lead to different length of summer blocking in Euro-Russian sector and the role of strong blocking episodes in favouring land surface feedbacks and in affecting heat waves durations.

Supporting information

The following supporting information is available:

Figure S1. Probability Distribution Function of length (days) of Euro-Russian blocking in NCEP Reanalysis for the periods 1961–2010 (thick line, see Figure 3), 1960–1980 (Blue line) and 1990–2010 (Red line). PDF's are computed by adopting a Gaussian kernel function estimator and by using a window parameter

$h = 3.5*0$, where 0 is the bin amplitude. (b) Difference of PDFs for the length of blocking events between the 1990–2010 and 1960–1980 periods. If the Kolmogorov–Smirnov test (KS) = 1, the differences in the length of blocking events are significant at the 99% confidence level (KS = 0 otherwise).

Acknowledgements

References

Anderson JL. 1993. The climatology of blocking in a numerical forecast model. *Journal of Climate* **6**: 1041–1056.

Atlas R, Wolfson N, Terry J. 1993. The effects of SST and soil moisture anomalies on GLA model simulations of the 1988 US summer drought. *Journal of Climate* **6**: 2034–2048, DOI: 10.1175/1520-0442.

Barriopedro D, Fischer EM, Luterbacher J, Trigo RM, García-Herrera R. 2011. The hot summer of 2010: redrawing the temperature record map of Europe. *Science* **332**: 220–224, DOI: 10.1126/science.1201224.

Black E, Blackburn M, Harrison G, Hoskins B, Methven J. 2004. Factors contributing to the summer 2003 European heatwave. *Weather* **59**: 217–223, DOI: 10.1256/wea.74.04.

Carillo A, Ruti PM, Navarra A. 2000. Storm tracks and zonal mean flow variability: a comparison between observed and simulated data. *Climate Dynamics* **16**(2–3): 219–228, DOI: 10.1007/s003820050015.

Cassou C, Terray L, Phillips AS. 2005. Tropical Atlantic influence on European heat waves. *Journal of Climate* **18**: 2805–2811.

Cattiaux J, Yiou P, Vautard R. 2012. Dynamics of future seasonal temperature trends and extremes in Europe: a multi-model analysis from CMIP3. *Climate Dynamics* **38**, DOI: 10.1007/s00382-011-1211-1.

Corti S, Molteni F, Palmer TN. 1999. Signature of recent climate change in frequencies of natural atmospheric circulation regimes. *Nature* **398**: 799–802.

D'Andrea F, Tibaldi S, Blackburn M, Boer G, Déqué M, Dugas B, Ferranti L, Hunt B, Iwasaki T, Kitoh A, Pope V, Randall D, Roeckner E, Straus D, Stern W, Van den Dool H, Williamson D. 1998. Northern hemisphere atmospheric blocking as simulated by 15 atmospheric general circulation models in the period 1979–1988. *Climate Dynamics* **4**: 385–407.

Dell'Aquila A, Lucarini V, Ruti PM, Calmanti S. 2005. Hayashi spectra of the Northern Hemisphere mid-latitude atmospheric variability in the NCEP-NCAR and ECMWF reanalyses. *Climate Dynamics*: 639–652, DOI: 10.1007/s00382-005-0048-x.

Doblas-Reyes FJ, Casado MJ, Pastor MA. 2002. Sensitivity of the northern hemisphere blocking frequency to the detection index. *Journal of Geophysical Research* **107**, DOI: 10.1029/2000JD000290.

Dole R, Hoerling M, Perlwitz J, Eischeid J, Pegion P, Zhang T, Quan XW, Xu T, Murray D. 2011. Was there a basis for anticipating the 2010 Russian heat wave? *Geophysical Research Letters* **38**: L06702, DOI: 10.1029/2010GL046582.

Dunn-Sigouin E, Son SW. 2013. Northern Hemisphere blocking frequency and duration in the CMIP5 models. *Journal of Geophysical Research – Atmospheres* **118**: 1179–1188, DOI: 10.1002/jgrd.50143.

Ferranti L, Molteni F, Palmer TN. 1994. Impact of localised tropical and extra tropical SST anomalies in ensembles of seasonal GCM integrations. *Quarterly Journal of the Royal Meteorological Society* **120**: 1613–1645.

Fischer EM, Seneviratne SI, Lüthi D, Schär C. 2007. Contribution of land–atmosphere coupling to recent European summer heat waves. *Geophysical Research Letters* **34**: L06707, DOI: 10.1029/2006GL029068.

Fischer EM, Rajczak J, Schär C. 2012. Changes in European summer temperature variability revisited. *Geophysical Research Letters* **39**: L19702, DOI: 10.1029/2012GL052730.

Hansen AR, Sutera A. 1986. On the probability density distribution of planetary-scale atmospheric wave amplitude. *Journal of the Atmospheric Sciences* **43**: 3250–3265.

IPCC, Intergovernmental Panel on Climate Change. 2001. Climate change 2001: The scientific basis. In *Contribution of Working Group I to the Third Assessment Report of the Intergovernmental Panel on Climate Change*, Houghton JT, Ding Y, Griggs DJ, Noguer M, van der Linden PJ, Dai X, Maskell K, Johnson CA (eds). Cambridge University Press: Cambridge; 881.

Jung T. 2005. Systematic errors of the atmospheric circulation in the ECMWF forecasting system. *Quarterly Journal of the Royal Meteorological Society* **131**: 1045–1073.

Lupo AR, Oglesby RJ, Mokhov II. 1997. Climatological features of blocking anticyclones: a study of Northern Hemisphere CCM1 model blocking events in present-day and double CO2 concentrations. *Climate Dynamics* **13**: 181–195.

Matsueda M, Mizuta R, Kusunoki S. 2009. Future change in wintertime atmospheric blocking simulated using a 20-km mesh atmospheric global circulation model. *Journal of Geophysical Research* **114**: D12114, DOI: 10.1029/2009JD011919.

Petoukhov V, Rahmstorf S, Petri S, Schellnhuber HJ. 2013. Quasi-resonant amplification of planetary waves and recent Northern Hemisphere weather extremes. *PNAS*, DOI: 10.1073/pnas.1222000110.

Rayner NA, Parker DE, Horton EB, Folland CK, Alexander LV, Rowell DP, Kent EC, Kaplan A. 2003. Global analyses of sea surface temperature, sea ice, and night marine air temperature since the late nineteenth century. *Journal of Geophysical Research* **108**(D14): 4407, DOI: 10.1209/2002JD002670.

Ruti PM, Lucarini V, Dell'Aquila A, Calmanti S, Speranza A. 2006. Does the subtropical jet catalyze the midlatitude atmospheric regimes? *Geophysical Research Letters* **33**: L06814, DOI: 10.1029/2005GL024620.

Scaife AA, Copsey D, Gordon C, Harris C, Hinton TJ, Keeley SPE, O'Neill A, Roberts MJ, Williams KD. 2011. Improved Atlantic winter blocking in a climate model. *Geophysical Research Letters*, DOI: 10.1029/2011GL049573.

Schär C, Vidale PL, Lüthi D, Frei C, Häberli C, Liniger M, Appenzeller C. 2004. The role of increasing temperature variability in European summer heat waves. *Nature* **427**: 332–336.

Tibaldi S, Molteni F. 1990. On the operational predictability of blocking. *Tellus A* **42**: 343–365.

Tibaldi S, Ruti P, Tosi E, Maruca MM. 1995. Operational predictability of winter blocking. *Annals of Geophysics* **13**: 305–317.

Vial J, Osborn TJ. 2011. Assessment of atmosphere–ocean general circulation model simulations of winter northern hemisphere atmospheric blocking. *Climate Dynamics*, DOI: 10.1007/s00382-011-1177-z.